Measuring Lyapunov exponents of large chaotic systems with global coupling by time series analysis

Taro P. Shimizu, and Kazumasa A. Takeuchi

Measuring Lyapunov exponents of large chaotic systems with global coupling by time series analysis

Taro P. Shimizu[1] and Kazumasa A. Takeuchi[1,2]

[1]*Department of Physics, Tokyo Institute of Technology, 2-12-1 Ookayama, Meguro-ku, Tokyo 152-8551, Japan*
[2]*Department of Physics, The University of Tokyo, 7-3-1 Hongo, Bunkyo-ku, Tokyo 113-0033, Japan*

Despite the prominent importance of the Lyapunov exponents for characterizing chaos, it still remains a challenge to measure them for large experimental systems, mainly because of the lack of recurrences in time series analysis. Here, we develop a method to overcome this difficulty, valid for highly symmetric systems such as systems with global coupling, for which the dimensionality of recurrence analysis can be reduced drastically. We test our method numerically with two globally coupled systems, namely, logistic maps and limit-cycle oscillators with global coupling. The evaluated exponent values are successfully compared with the true ones obtained by the standard numerical method. We also describe a few techniques to improve the accuracy of the proposed method. *Published by AIP Publishing.* https://doi.org/10.1063/1.5066087

Although chaos with many degrees of freedom abounds in a wide variety of natural systems, such as turbulence in geophysical flows and laboratory experiments,[1] chemical reactions,[2] and possibly cardiac arrhythmia,[3] it still remains challenging to characterize their instability in a quantitative manner. A practical method for measuring Lyapunov exponents is particularly called for, because the Lyapunov exponents and related concepts are useful to characterize various aspects of chaos, as well as for application purposes such as chaos control.[4] In this work, we propose a method to evaluate the Lyapunov exponents of large chaotic systems from time series, which is valid for systems with a high degree of symmetry. Focusing on globally coupled systems, and using a time series of a single local variable and the mean field, we demonstrate that our method can indeed estimate the full spectrum of the Lyapunov exponents correctly. We expect that the presented idea can also be extended to other types of symmetric systems, paving the way toward experimental investigations of instability of large chaotic systems in the future.

I. INTRODUCTION

Instability is one of the most fundamental properties of nonlinear dynamical systems. It is often characterized by the Lyapunov exponents, i.e., the exponential rates of divergence of infinitesimal perturbations given to a trajectory. The Lyapunov exponents are also known to characterize properties of chaotic systems other than instability, such as the metric entropy and the attractor dimension.[5] Moreover, for large systems, the extensivity of chaos is defined on the basis of the spectrum of the Lyapunov exponents.[6] From the application point of view, the Lyapunov exponents and related objects play an important role in chaos control[7] and data assimilation.[8] It is therefore not surprising that the Lyapunov exponents have been the central quantities to investigate in numerical studies of chaos, in which case the equation of motion is usually given and the methods to evaluate the exponents are established.[9–11] However, experimentally, the situation is in sharp contrast, because the equation of motion is usually unavailable and one often needs to resort to time series to estimate the Lyapunov exponents.

The most common experimental approach is the following:[4,9,12] (i) First, time series, say $s(t)$, is embedded to a space of sufficiently high dimensionality, by use of time-delayed coordinates $\boldsymbol{s}(t) = [s(t), s(t-\tau), s(t-2\tau), \ldots]$. (ii) Recurrences of trajectories, i.e., pairs of $\boldsymbol{s}(t_i)$ and $\boldsymbol{s}(t_j)$ with small $||\boldsymbol{s}(t_i) - \boldsymbol{s}(t_j)||$ are detected and the growth rate of $||\boldsymbol{s}(t_i + t) - \boldsymbol{s}(t_j + t)||$ is measured. Although this method works well for systems with a small number of degrees of freedom, it cannot be applied to large systems whose number of degrees of freedom is large (typically $\gtrsim 10$), because recurrence becomes extremely rare in such high-dimensional space. Recently, Pathak *et al.* used a machine learning technique to time series data and succeeded in predicting trajectories and even Lyapunov exponents of a large spatially-extended system.[13] This is an encouraging development, but adjusting many parameters involved in this method, without guiding principles, is presumably a delicate task in practice.

In this work, we choose to extend the recurrence method and attempt to overcome the problem of the lack of recurrences in large systems. Here, we restrict our target to a specific kind of systems, namely, systems with global coupling, but we believe that our method can be extended to other types of systems with a high degree of symmetry. We focus on the fact that the evolution of a local variable does not necessarily require a large number of variables; in the case of globally coupled systems, it is determined only by the local variable and the mean field. We therefore collect recurrences with this local set of variables and show that it is sufficient to construct the global Jacobian, which is necessary to compute the full spectrum of the Lyapunov exponents. We apply our method to two globally-coupled systems, specifically, logistic maps and limit-cycle oscillators with global coupling, and demonstrate that this method is able to evaluate the Lyapunov

spectrum reasonably well. We also describe a few techniques to improve the accuracy of the proposed method.

II. METHOD

Here, we describe our method for globally coupled systems in a general manner. For simplicity, it is described for the case in which the local evolution is given by a one-dimensional map, but generalization to higher dimensions and to differential equations is straightforward.

Consider a globally coupled system given by

$$x_j(t+1) = f(x_j(t), m(t)) \tag{1}$$

with $j = 1, 2, \ldots, N$, where $f(x, m)$ is a nonlinear map, $x_j(t)$ represents the jth local variable at discrete time t, $m(t)$ is the mean field given by

$$m(t) := \frac{1}{N} \sum_{j=1}^{N} x_j(t). \tag{2}$$

The full Jacobian matrix for this system is

$$
\begin{aligned}
&J(x_1(t), \ldots, x_N(t)) \\
&= \begin{bmatrix}
\frac{\partial}{\partial x_1} f(x_1(t), m(t)), & \cdots, & \frac{\partial}{\partial x_N} f(x_1(t), m(t)) \\
\vdots & & \vdots \\
\frac{\partial}{\partial x_1} f(x_N(t), m(t)), & \cdots, & \frac{\partial}{\partial x_N} f(x_N(t), m(t))
\end{bmatrix}.
\end{aligned} \tag{3}
$$

Here, note that the function $f(x, m)$ takes two independent arguments x and m, but since $m(t)$ is given by Eq. (2), the derivative in Eq. (3) should read

$$
\begin{aligned}
&\frac{\partial}{\partial x_i} f(x_j(t), m(t)) \\
&= \delta_{ij} \frac{\partial f}{\partial x}(x_j(t), m(t)) + \frac{1}{N} \frac{\partial f}{\partial m}(x_j(t), m(t))
\end{aligned} \tag{4}
$$

with Kronecker's delta δ_{ij}. An important observation here is that the full Jacobian is determined only by the two derivatives of the local map, $\frac{\partial f}{\partial x}$ and $\frac{\partial f}{\partial m}$. Therefore, time series data of a *single* local variable $x_1(t)$ and the mean field $m(t)$ are actually sufficient to reconstruct the full Jacobian matrix J.

We now describe the method. Assume that we have time series of a single local variable $x_1(t)$ and the mean field $m(t)$. With $\boldsymbol{p}_1(t) := [x_1(t), m(t)]^T$, the total derivative of Eq. (1) is

$$dx_1(t+1) = \begin{bmatrix} A(\boldsymbol{p}_1(t)), & B(\boldsymbol{p}_1(t)) \end{bmatrix} d\boldsymbol{p}_1(t), \tag{5}$$

where we define

$$
\begin{aligned}
A(\boldsymbol{p}_1(t)) &:= \frac{\partial f}{\partial x}(x_1(t), m(t)), \\
B(\boldsymbol{p}_1(t)) &:= \frac{\partial f}{\partial m}(x_1(t), m(t)).
\end{aligned} \tag{6}
$$

Note that Eq. (5) is equivalent to the evolution of an infinitesimal perturbation $dx_1(t)$ in a system with two *independent* variables $x_1(t)$ and $m(t)$, defined by Eq. (1). Therefore, we can use the standard recurrence method for this two-dimensional *reduced* space spanned by $x_1(t)$ and $m(t)$, and obtain the 1×2 matrix $[A(\boldsymbol{p}_1(t)), B(\boldsymbol{p}_1(t))]$ which we shall call the pseudo-local Jacobian matrix. Specifically, adapting the method proposed by Sano and Sawada[14] and by Eckmann and

Ruelle,[5,15] we use pairs of recurrent points $\boldsymbol{p}_1(t_i)$ and $\boldsymbol{p}_1(t_j)$, regard $d\boldsymbol{p}_1(t) \approx \boldsymbol{p}_1(t_i) - \boldsymbol{p}_1(t_j)$ and $dx_1(t+1) \approx x_1(t_i+1) - x_1(t_j+1)$, and evaluate the matrix $[A(\boldsymbol{p}_1(t)), B(\boldsymbol{p}_1(t))]$ by the least squares method. Importantly, here, we are able to obtain enough recurrences because the dimensionality of this reduced space is only two (or multiples of two if the local variable $x_j(t)$ is multidimensional). Then, with Eqs. (4) and (6), we obtain the Jacobian matrix (3) for the full system by appropriately interpolating $\frac{\partial f}{\partial x}(x, m)$ and $\frac{\partial f}{\partial m}(x, m)$.

To be precise, from time series data $\boldsymbol{p}_1(t) = [x_1(t), m(t)]^T$, we evaluate the Lyapunov exponents by the following two steps. *Step I.* We estimate the pseudo-local Jacobian matrix $[A(\boldsymbol{p}_1(t)), B(\boldsymbol{p}_1(t))]$ by recurrences of time series $\boldsymbol{p}_1(t)$ in the reduced space. To detect recurrences, we consider a small ball of radius ϵ centered at a given $\boldsymbol{p}_1(t)$, and obtain the set of the indices of the recurrences, $I_\epsilon(t) := \{t'; \|\boldsymbol{p}_1(t) - \boldsymbol{p}_1(t')\| < \epsilon\}$. Then, by the least squares method as described above, we obtain an estimate of the pseudo-local Jacobian matrix, denoted by $[\tilde{A}(\boldsymbol{p}_1(t)), \tilde{B}(\boldsymbol{p}_1(t))]$. *Step II.* We numerically emulate both phase-space and tangent-space dynamics by interpolating the functions $f(x, m)$, $\frac{\partial f}{\partial x}(x, m)$, and $\frac{\partial f}{\partial m}(x, m)$, from time series data for $x_1(t+1) = f(x_1(t), m(t))$, $\tilde{A}(\boldsymbol{p}_1(t)) \approx \frac{\partial f}{\partial x}(x_1(t), m(t))$, and $\tilde{B}(\boldsymbol{p}_1(t)) \approx \frac{\partial f}{\partial m}(x_1(t), m(t))$, respectively. Then, the Lyapunov exponents are obtained by the standard QR decomposition method.[9–11]

In the next two sections, we test our method with numerically generated time series, using globally coupled logistic maps (Sec. III) and globally coupled limit-cycle oscillators (Sec. IV).

III. GLOBALLY COUPLED LOGISTIC MAPS

A. System

We first consider a system of globally coupled logistic maps

$$
\begin{aligned}
x_j(t+1) &= f(X_j(t)), \\
X_j(t) &= (1-K)x_j(t) + Km(t)
\end{aligned} \tag{7}
$$

with $j = 1, 2, \ldots, N$, a coupling constant K, and the logistic map $f(x) = 1 - ax^2$. Then, the 1×2 pseudo-local Jacobian matrix $[A(\boldsymbol{p}_1(t)), B(\boldsymbol{p}_1(t))]$ is given by

$$
\begin{aligned}
A(\boldsymbol{p}_1(t)) &= (1-K)f'(X_1(t)), \\
B(\boldsymbol{p}_1(t)) &= Kf'(X_1(t)).
\end{aligned} \tag{8}
$$

In the following, we set $K = 0.1$, $a = 2$, and $N = 200$. This corresponds to a regime of high-dimensional chaos,[16] which does not show any apparent coherence in the values of the local variables (in particular, there is no synchronization at least in the usual sense). We assume that we know the system to analyze has a global coupling in the additive form, as expressed generically by Eq. (7), but that the function $f(x)$ is unknown. We used time series data of a local variable $x_1(t)$ and the mean field $m(t)$, generated numerically after discarding a transient. The length of the time series data was $T = 10^5$. We applied our method described in Sec. II. The radius of the ϵ-ball neighborhood was set to $\epsilon = 10^{-2}$.
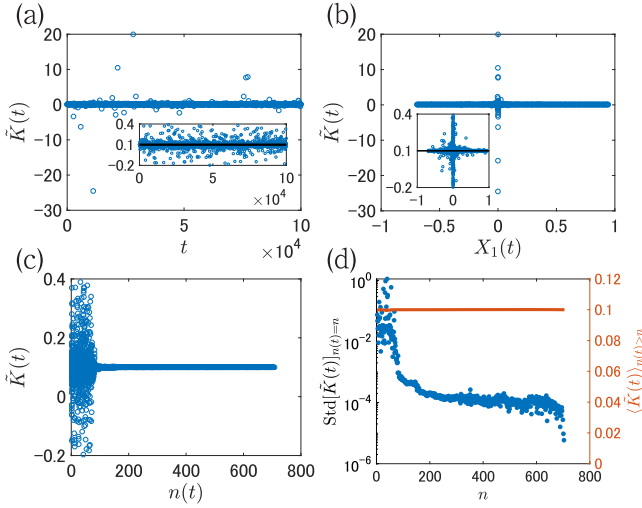
FIG. 1. Estimation of the coupling constant K for the globally coupled logistic maps. (a) and (b) Estimates $\tilde{K}(t)$ shown against t (a) and $X_1(t)$ (b). The insets are close-ups showing the range $-0.4 \le \tilde{K}(t) \le 0.6$, with the true value $K = 0.1$ indicated by the black solid line. (c) Estimates $\tilde{K}(t)$ shown against the number of recurrences $n(t) := |I_\epsilon(\boldsymbol{p}_1(t))|$. (d) Standard deviation of the estimates $\tilde{K}(t)$ with $n(t) = n$ (blue dots) and the mean of $\tilde{K}(t)$ such that $n(t) > n$ (orange line) shown against n.

B. Results

First, following Step I described in Sec. II, we evaluate the coupling constant K. Using Eq. (7), we have $K = B(\boldsymbol{p}_1(t))/(A(\boldsymbol{p}_1(t)) + B(\boldsymbol{p}_1(t)))$. Therefore, from the estimates $(\tilde{A}(\boldsymbol{p}_1(t)), \tilde{B}(\boldsymbol{p}_1(t)))$ of the pseudo-local Jacobian matrix, we obtain estimates of K,

$$\tilde{K}(t) = \frac{\tilde{B}(\boldsymbol{p}_1(t))}{\tilde{A}(\boldsymbol{p}_1(t)) + \tilde{B}(\boldsymbol{p}_1(t))}. \tag{9}$$

Note that, though the true coupling parameter K is a constant, it is evaluated for each data point $\boldsymbol{p}_1(t)$ so that $\tilde{K}(t)$ is a function of t.

Figure 1(a) shows $\tilde{K}(t)$ as a function of time. By taking the time average, we obtain $\langle \tilde{K}(t) \rangle \approx 0.09998$, which differs from the true value $K = 0.1$ only by the order of 10^{-5}. However, the standard deviation of $\tilde{K}(t)$ is actually as large as 0.13, which is also apparent from scattered data points in Fig. 1(a).

A closer look reveals that errors are anomalously large when $X_1(t) \approx 0$ [Fig. 1(b)]. This is easy to understand because $f'(X_1(t)) = -2aX_1(t)$ is then almost vanishing and so is $dx_1(t+1)$ given by Eqs. (5) and (8).

Therefore, the estimation of $[\tilde{A}(\boldsymbol{p}_1(t)), \tilde{B}(\boldsymbol{p}_1(t))]$, or equivalently that of $\tilde{K}(t)$ and $\tilde{f}'(X_1(t))$, becomes numerically unstable for those particular data points. The remaining source of error is the lack of recurrences. In Fig. 1(c), the estimates $\tilde{K}(t)$ are plotted against $n(t) := |I_\epsilon(\boldsymbol{p}_1(t))|$, i.e., the number of the recurrence points around the data point $\boldsymbol{p}_1(t)$. It is clear that large errors are essentially originated from data points with small n. This is quantified in Fig. 1(d), which shows how the standard deviation of $\tilde{K}(t)$ with a given number of recurrences n, denoted by $\mathrm{Std}[\tilde{K}(t)]_{n(t)=n}$, decreases with increasing n (blue dots). We can see that the error level becomes very low, in the order of 10^{-4}, for $n \gtrsim 100$. Errors are not negligible for smaller n, but even so, the number of such data points is small enough so that the mean of $\tilde{K}(t)$ such that $n(t) > n$, denoted by $\langle \tilde{K}(t) \rangle_{n(t)>n}$, is hardly affected by the choice of the threshold n [orange line in Fig. 1(d)].

In any case, we obtain a reasonable estimate for the coupling constant, $\tilde{K} := \langle \tilde{K}(t) \rangle \approx 0.09998$. The derivative $f'(X)$ is evaluated, from (8), by $\tilde{f}'(\tilde{X}_1(t)) = \tilde{A}(\boldsymbol{p}_1(t)) + \tilde{B}(\boldsymbol{p}_1(t))$ with $\tilde{X}_1(t) := (1-K)x_1(t) + \tilde{K}m(t)$. Then, we carry out Step II in Sec. II and evaluate the Lyapunov exponents. Figure 2 shows the result (blue circles), compared with the true spectrum (black line) which we obtain directly by applying the QR decomposition method to the globally coupled logistic maps. It is confirmed that our method successfully evaluated the Lyapunov exponents in the entire spectrum.

IV. GLOBALLY COUPLED LIMIT CYCLE OSCILLATOR

A. System

For the second example, we choose a system with continuous time, specifically a system of limit-cycle oscillators with global coupling, defined as follows:

$$\dot{w}_j(t) = w_j(t) - (1 + c_2)|w_j(t)|^2 w_j(t)$$
$$+ K(1 + \mathrm{i}c_1)(\bar{w}(t) - w_j(t)) \tag{10}$$

with $j = 1, 2, \ldots, N$, complex variables $w_j(t)$, the mean field $\bar{w}(t) := (1/N)\sum_j w_j(t)$, a coupling constant K, and system parameters c_1, c_2. To write down the pseudo-local Jacobian matrix, it is convenient to use $x_j(t) := \mathrm{Re}[w_j(t)]$ and $y_j(t) := \mathrm{Im}[w_j(t)]$, and discretize time by the Euler method with time step Δt. The resulting submatrices $A(\boldsymbol{p}_1(t))$ and $B(\boldsymbol{p}_1(t))$, which are now 2×2 with $\boldsymbol{p}_1(t) := [x_1(t), y_1(t), \bar{x}(t), \bar{y}(t)]^T$, read

$$A(\boldsymbol{p}_1(t)) = \begin{bmatrix} 1 - 3x_1^2(t) - y_1^2(t) + 2c_2 x_1(t)y_1(t) - K, & c_2 x_1^2(t) + 3c_2 y_1^2(t) - 2x_1(t)y_1(t) + Kc_1 \\ -3c_2 x_1^2(t) - c_2 y_1^2(t) - 2x_1(t)y_1(t) - Kc_1, & 1 - x_1^2(t) - 3y_1^2(t) - 2c_2 x_1(t)y_1(t) - K \end{bmatrix} \Delta t + \begin{bmatrix} 1 & 0 \\ 0 & 1 \end{bmatrix},$$

$$B(\boldsymbol{p}_1(t)) = \begin{bmatrix} K & -Kc_1 \\ Kc_1 & K \end{bmatrix} \Delta t. \tag{11}$$

In the following, we set $K = 0.52$, $c_1 = -2.5$, $c_2 = 3.0$, which correspond to a regime of high-dimensional chaos,[17,18] and the system size is set to be $N = 50$. Again, the oscillators are not synchronized, but distributed in the complex plane.[17,18]

For the analysis, we assume that we know the target is a system described in the following form:

$$\dot{x}_j(t) = f_x(x_j(t), y_j(t)) + K_{xx}(\bar{x}(t) - x_j(t)) + K_{xy}(\bar{y}(t) - y_j(t)),$$
$$\dot{y}_j(t) = f_y(x_j(t), y_j(t)) + K_{yx}(\bar{x}(t) - x_j(t)) + K_{yy}(\bar{y}(t) - y_j(t)), \tag{12}$$
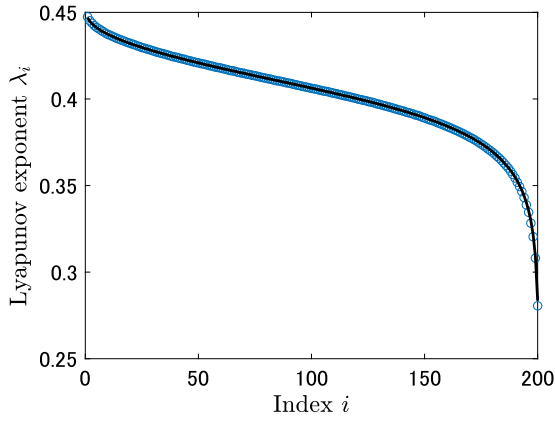
FIG. 2. The spectrum of the Lyapunov exponents λ_i for the globally coupled logistic maps, evaluated by the proposed method (blue circles). The black line indicates the true spectrum obtained by the standard QR decomposition method.

but the functional forms of $f_x(x, y)$ and $f_y(x, y)$, as well as the values of the four coupling constants are unknown. The pseudo-local Jacobian matrix then reads

$$A(x_1, y_1) = \begin{bmatrix} \frac{\partial f_x}{\partial x}(x_1, y_1) - K_{xx}, & \frac{\partial f_x}{\partial y}(x_1, y_1) - K_{xy} \\ \frac{\partial f_y}{\partial x}(x_1, y_1) - K_{yx}, & \frac{\partial f_y}{\partial y}(x_1, y_1) - K_{yy} \end{bmatrix} \Delta t$$

$$+ \begin{bmatrix} 1 & 0 \\ 0 & 1 \end{bmatrix},$$

$$B = \begin{bmatrix} K_{xx} & K_{xy} \\ K_{yx} & K_{yy} \end{bmatrix} \Delta t. \tag{13}$$

Note that, thanks to the linear coupling to the mean field, the matrix $A(\boldsymbol{p}_1)$ depends only on x_1 and y_1, and $B(\boldsymbol{p}_1)$ is a constant matrix.

We used time series of a local variable $w_1(t) = x_1(t) + iy_1(t)$ and the mean field $\bar{w}(t) = \bar{x}(t) + i\bar{y}(t)$, generated numerically by the fourth-order Runge-Kutta method with time step $\Delta t = 10^{-3}$, after discarding a transient. The length of the time series data was $T = 10^6$ (in the unit of time step). Then, we applied our method with $\epsilon = 10^{-2}$ and evaluated the coupling constants and the Lyapunov exponents.

B. Results

Similarly to the procedure we adopted in Sec. III, by Step I, we first evaluate the coupling constants. Taking K_{xx} as an example, from Eq. (13), we obtain $\tilde{K}_{xx}(t) = \tilde{B}(\boldsymbol{p}_1(t))/\Delta t$ [Fig. 3(a)]. The data suggest that, compared to the previous case, the estimates $\tilde{K}_{xx}(t)$ tend to meander far from the true value $K_{xx} = K = 0.52$ for longer time. Indeed, simple time averaging now yields a totally wrong value, $\langle \tilde{K}_{xx}(t) \rangle \approx 6.08$. On the other hand, we find that the median gives a reasonable value 0.515, suggesting that $\tilde{K}_{xx}(t)$ still spends much time near the true value [see also the inset of Fig. 3(a)].

The estimation accuracy can be improved by paying attention to the number of recurrences. Figures 3(b) and 3(c) display $\tilde{K}_{xx}(t)$ against $n(t) = |I_\epsilon(\boldsymbol{p}_1(t))|$ [panel (b)], as well as $\mathrm{Std}[\tilde{K}_{xx}(t)]_{n(t)=n}$ [blue dots of panel (c)] and $\langle \tilde{K}_{xx}(t) \rangle_{n(t)>n}$
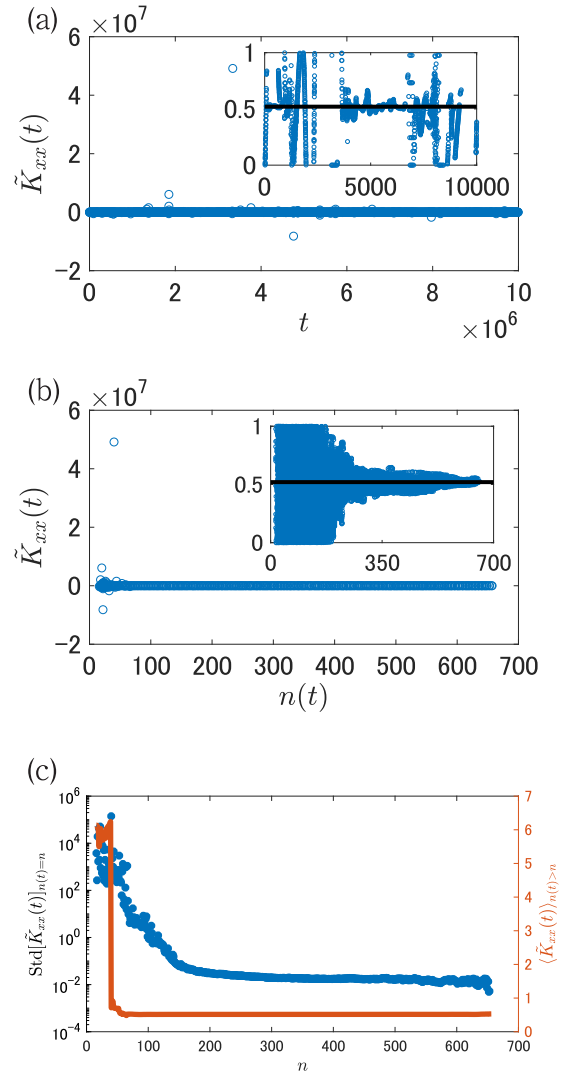

FIG. 3. Estimation of the coupling constant K_{xx} for the globally coupled limit-cycle oscillators. (a) and (b) Estimates $\tilde{K}_{xx}(t)$ shown against time t (a) and the number of recurrences $n(t) := |I_\epsilon(\boldsymbol{p}_1(t))|$ (b). The insets are close-ups showing the range $0 \leq \tilde{K}_{xx}(t) \leq 1$, with the true value $K = 0.52$ indicated by the black solid line. (c) Standard deviation of the estimates $\tilde{K}_{xx}(t)$ with $n(t) = n$ (blue dots) and the mean of $\tilde{K}_{xx}(t)$ such that $n(t) > n$ (orange line) shown against n.

(orange line) against n. These results consistently show that most errors in $\langle \tilde{K}_{xx}(t) \rangle$ are due to the data points with only few recurrent points. Therefore, we can improve the accuracy by setting a lower threshold for n, denoted by n_{trm}, and using only the data points with $n(t) > n_{\mathrm{trm}}$. We shall call this operation "trimming," and n_{trm} the trimming threshold. Figure 3(c) shows that, with $n_{\mathrm{trm}} \approx 50$, the mean estimate $\langle \tilde{K}_{xx}(t) \rangle_{n(t)>n}$ is already stable (orange line) but individual estimates $\tilde{K}_{xx}(t)$ are still fluctuating (blue dots). The fluctuation level becomes low for $n \gtrsim 200$ or 300 [see also Fig. 3(b)], so that these are expected to be an appropriate choice for the value of n_{trm}.

Now, we evaluate the Lyapunov exponents via Step II, i.e., by emulating the phase-space and tangent-space dynamics. The phase-space dynamics is realized by the time evolution equation (12). Here, for the coupling constants, the values obtained previously with the trimming technique are used, and the functions $f_x(x_j, y_j)$ and $f_y(x_j, y_j)$ are evaluated
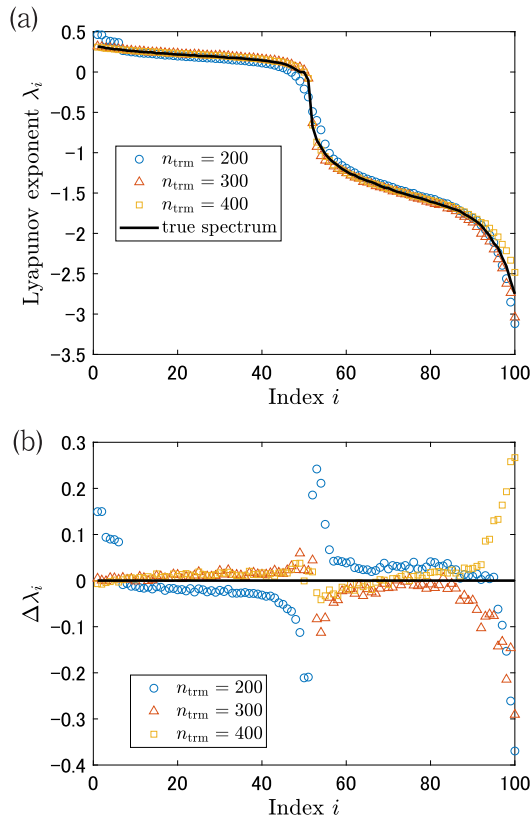
(a)

(b)

FIG. 4. The spectrum of the Lyapunov exponents λ_i for the globally coupled limit-cycle oscillators. (a) The spectrum evaluated by the proposed method (symbols) for different choices of the trimming threshold n_{trm}. The black line indicates the true spectrum λ_i^{true} obtained by the standard QR decomposition method. (b) The estimation error $\Delta\lambda_i := \lambda_i - \lambda_i^{\text{true}}$.

by interpolation of the time series data. The tangent-space dynamics is reconstructed by interpolating the estimates of the matrix $A(x_j, y_j)$ [Eq. (13)] while for B, the obtained values of the coupling constants are used. For those interpolations, we again need to have sufficiently many neighbors around each time-series data point. In fact, we can increase this number in the case where we know *a priori* that our oscillators are invariant under uniform shift of the phase, i.e., under the transformation $w_j(t) \rightarrow w_j(t)e^{i\theta}$ with a constant θ for all j. Specifically, if we are to evaluate $A(x_j, y_j)$, or equivalently $A(w_j)$, we only need to find $w_1(t)$ from the time series data such that the modulus $|w_1(t)|$ is close to $|w_j|$. Then, we rotate $w_1(t)$ by the angle $\theta = \arg w_j - \arg w_1(t)$, or, more precisely, transform $A(w_1(t))$ to $R(\theta)A(w_1(t))R^{-1}(\theta)$ with the rotation matrix $R(\theta) := \left(\begin{smallmatrix} \cos\theta & -\sin\theta \\ \sin\theta & \cos\theta \end{smallmatrix} \right)$, and interpolate the value on the one-dimensional number line. The interpolation of $f_x(x, y)$ and $f_y(x, y)$ can also be done analogously, for which we use the fourth-order central-difference formula to evaluate $\dot{w}_1$ from the time series $w_1(t)$.

Figure 4(a) shows the Lyapunov spectrum obtained by our method (symbols), with varying trimming threshold n_{trm}, compared with the true spectrum (black line), which is obtained by using the QR decomposition method to the limit-cycle oscillators (10). The difference from the true spectrum is displayed in Fig. 4(b). We can confirm that our results reproduce the true spectrum reasonably well.

V. CONCLUSIONS

In this work, we proposed a method to evaluate the Lyapunov exponents from time series data of large chaotic systems with global coupling. The central idea is to handle the recurrence analysis in the reduced space, which consists only of a local variable and the mean field, thus circumventing the usual difficulty of the lack of recurrence points. We demonstrated the validity of our method with two representative systems, namely, the globally coupled logistic maps and the globally coupled limit-cycle oscillators, and reproduced the true Lyapunov spectrum reasonably well. It is true that systems with global coupling, which we consider in this work, are a specific kind of large dynamical system. However, there are real examples of such systems, as shown by laboratory experiments of chaotic electrochemical oscillators[2] and metabolic oscillations of stirred yeast cells.[19] In general, well-mixed many-component systems can often be regarded as systems with global coupling. Those systems are potential targets for applying our method experimentally.

Compared to the recently proposed method based on the machine learning technique,[13] which does not require *a priori* assumptions on the form of coupling, the advantage of our method is that the adjustable parameters are much fewer: specifically, the cutoff ϵ for the detection of recurrences and the trimming threshold n_{trm}, whose physical meaning is also clear. Our method can also be extended to other types of systems that have a high degree of symmetry, in the sense that the evolution of a local dynamical variable is determined by a small number of variables. We are aware that, for applying our method to experimental systems, we also need to incorporate the embedding technique[4,9,12] as well as to evaluate the influence of noise and inhomogeneity—important tasks left for future studies. We believe that the results presented here make the first step on this track, toward the realization of instability analysis of large experimental systems.

[1]U. Frisch, *Turbulence: The Legacy of A. N. Kolmogorov* (Cambridge University Press, 1995).
[2]W. Wang, I. Z. Kiss, and J. Hudson, Chaos **10**, 248 (2000).
[3]E. M. Cherry, and F. H. Fenton, New J. Phys. **10**, 125016 (2008).
[4]E. Ott, *Chaos in Dynamical Systems*, 2nd ed. (Cambridge University Press, Cambridge, 2002).
[5]J.-P. Eckmann, and D. Ruelle, Rev. Mod. Phys. **57**, 617 (1985).
[6]D. Ruelle, Commun. Math. Phys. **87**, 287 (1982).
[7]B. Andrievskii, and A. Fradkov, Autom. Remote Control **65**, 505 (2004).
[8]N. Balci, A. L. Mazzucato, J. M. Restrepo, and G. R. Sell, Mon. Weather Rev. **140**, 2308 (2012).
[9]A. Pikovsky, and A. Politi, *Lyapunov Exponents: A Tool to Explore Complex Dynamics* (Cambridge University Press, 2016).
[10]I. Shimada, and T. Nagashima, Prog. Theor. Phys. **61**, 1605 (1979).
[11]G. Benettin, L. Galgani, A. Giorgilli, and J.-M. Strelcyn, Meccanica **15**, 9 (1980).
[12]H. Kantz, and T. Schreiber, *Nonlinear Time Series Analysis* (Cambridge University Press, 2004), Vol. 7.
[13]J. Pathak, Z. Lu, B. R. Hunt, M. Girvan, and E. Ott, Chaos **27**, 121102 (2017).

[14]M. Sano, and Y. Sawada, Phys. Rev. Lett. **55**, 1082 (1985).

[15]J.-P. Eckmann, S. O. Kamphorst, D. Ruelle, and S. Ciliberto, Phys. Rev. A **34**, 4971 (1986).

[16]K. Kaneko, Physica D **41**, 137 (1990).

[17]N. Nakagawa, and Y. Kuramoto, Physica D **75**, 74 (1994).

[18]N. Nakagawa, and Y. Kuramoto, Physica D **80**, 307 (1995).

[19]S. De Monte, F. d'Ovidio, S. Danø, and P. G. Sørensen, Proc. Natl. Acad. Sci. U.S.A. **104**, 18377 (2007).